Impact of dust grain geometry on nebular emission around evolved stars





P. Jiménez-Hernández¹, S. J. Arthur², Daniel Guirado³, Olga Muñoz³, Julia Martikainen³ and L. Sabin¹ ¹Instituto de Astronomía, UNAM; ²Instituto de Radioastronomía y Astrofísica, UNAM; ³Instituto de Astrofísica de Andalucía (IAA-CSIC).

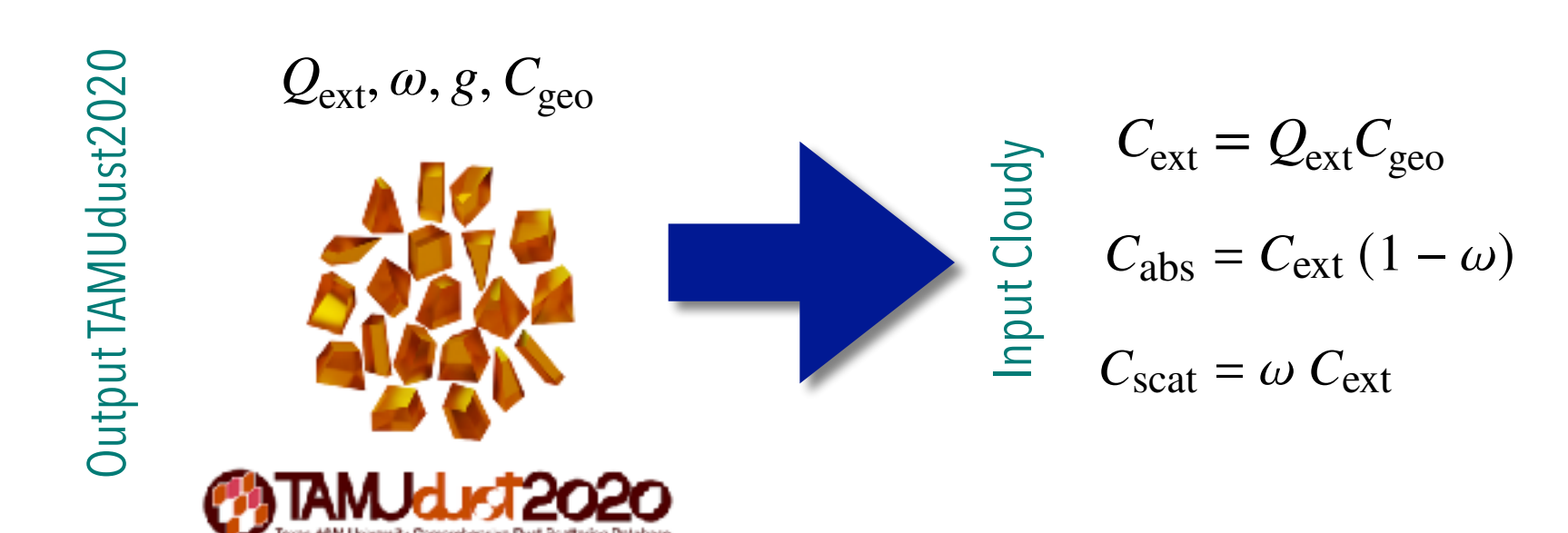
pajimenez@astro.unam.mx

Outline

Dust grains in circumstellar nebulae around evolve stars reprocess the stellar radiation and are responsible for the emission at mid-infrared (MIR) to far-infrared (FIR) wavelengths. Simplifications made regarding the grain shapes lead to difficulties in interpreting the infrared (IR) spectral energy distributions (SEDs) and spectra of nebulae around evolved stars. For example, in order to model the long wavelength IR SEDs of some circumstellar nebulae, authors have had to postulate extremely high dust-to-gas ratios, very large grain sizes or a high degree of porosity in order to reproduce the observation. We study the effects of using the optical properties of irregular hexahedral grains in photoionization models of nebulae around a WR star.

Methods

Dust opacities for the irregular grains were obtained from the scattering properties available in the TAMUdust2020 database [1] and these were implemented in the spectral synthesis code Cloudy [2]. Fig 1 shows the data obtained for the particular case of graphite dust composition.



A sample of photoionization models that use opacities from both spherical and irregular hexahedral grains across a standard MRN power law size distribution (0.005–0.25 μ m) was produced. We consider the optical properties of graphite, amorphous carbon and silicate dust grains dividing the full size range into 10 bins (see Tab 1) enables us to differentiate the contributions of small grains (which absorb most of the radiation) from those of the large grains (which contain most of the mass).

Bin	B ₁	B_2	B ₃	B ₄	B ₅	B ₆	B ₇	B ₈	B ₉	B ₁₀
$a_{\min} [\mu m]$	0.00500	0.00739	0.01093	0.01617	0.02319	0.03536	0.05228	0.07731	0.11433	0.16906
$a_{\rm max} [\mu {\rm m}]$	0.00739	0.01093	0.01617	0.02319	0.03536	0.05228	0.07731	0.11433	0.16906	0.25000

Tab 1. Smallest (a_{min}) and larger (a_{max}) grains size in each bin within the total size distribution.

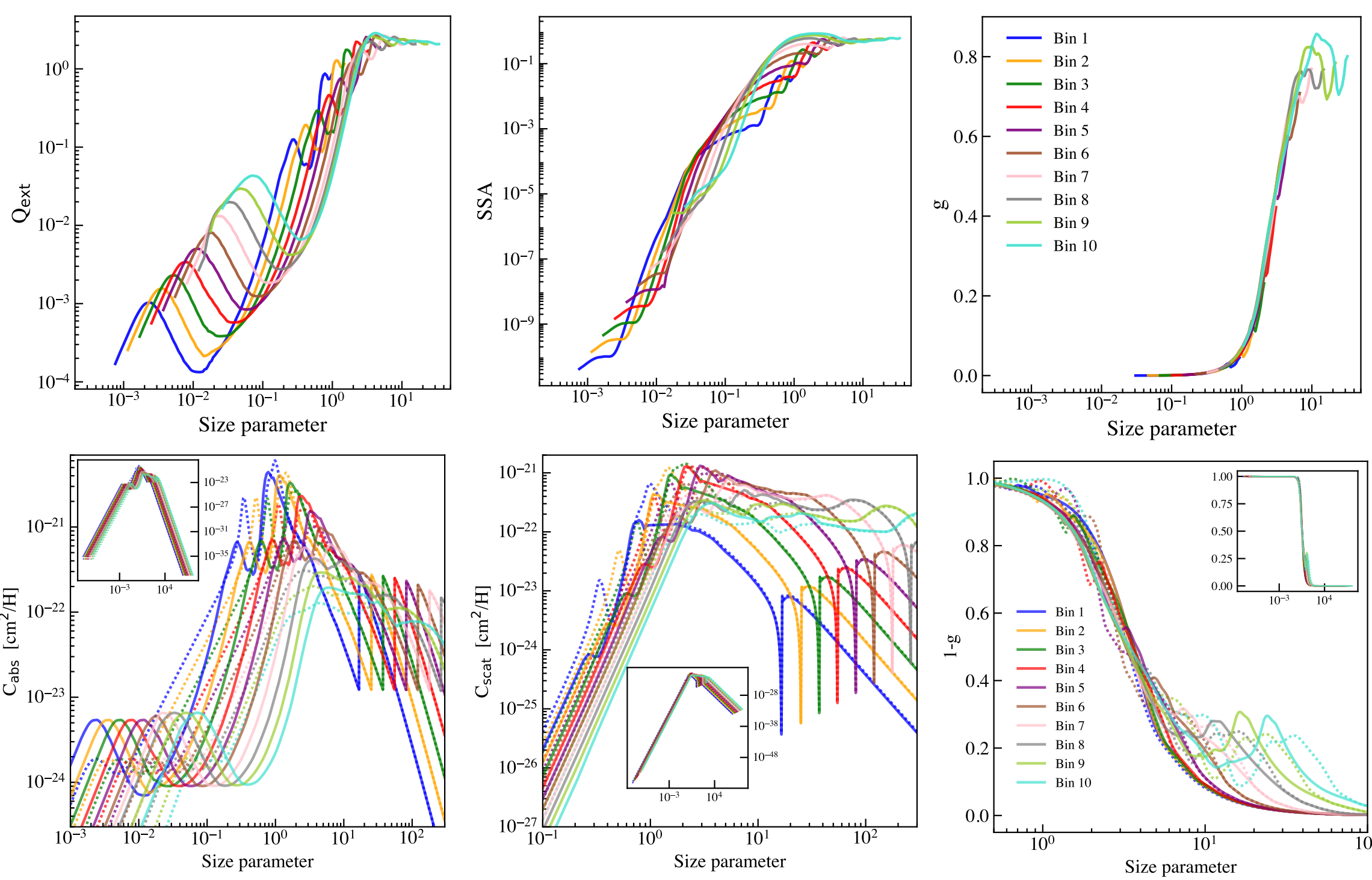


Fig 1. Top - output TAMUdust2020: Extinction efficiency (Q_{ext}), single-scattering albedo (ω), and asymmetry factor (g) for graphite grains from the TAMUdust2020 database, computed over 10 size bins (Table 1). Bottom - Input Cloudy: Opacity parameters for graphite grains computed for two grain shapes: hexahedral (solid lines) and spherical (dotted lines), across the same size bins. Left: Absorption cross section (Cabs) per H nucleon. Middle: Scattering cross section (C_{scat}) per H nucleon. Right: 1 - g values.

Photoionization Models

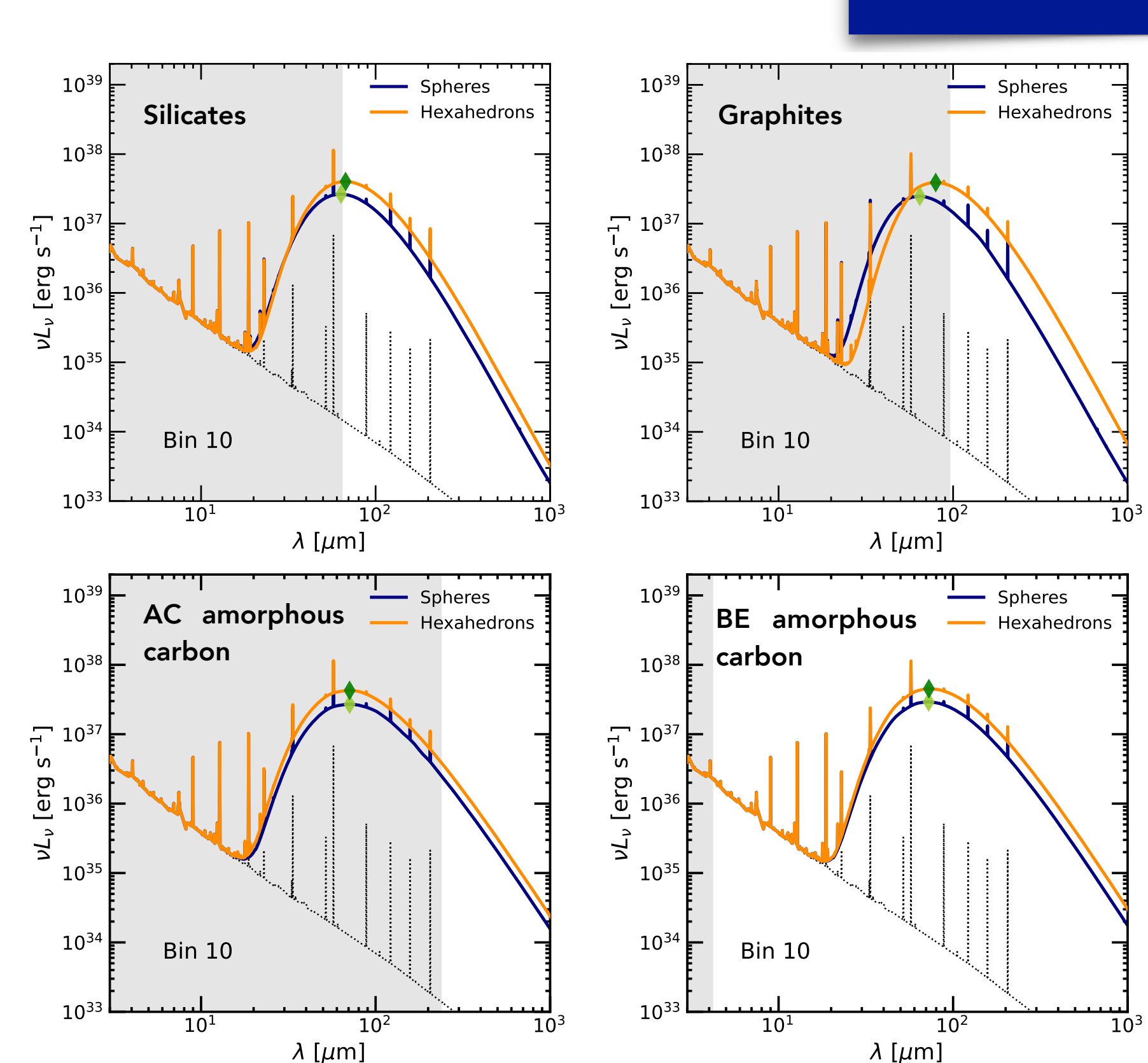


Fig 2. Spectra from Cloudy models, comparing spherical (blue line) and hexahedralshaped (orange line) grains. The panels show models using only the grain sizes corresponding to bin size 10.

The photoionization code Cloudy allows us to treat the interaction between the UV flux from the central star and the nebular gas and dust consistently. For the spectrum of the central stars we used PoWR stellar atmosphere models [3].

The differences between the model nebula continua calculated using spherical and irregular dust grains increase with the grain size, especially for graphite, see Fig 2.

Main findings

Continuum Shift: Irregular hexahedral grains shift the dust continuum to longer wavelengths and enhance far-IR fluxes relative to spherical models (see Fig 2).

Model Implications: This effect reproduces observed far-IR emission without invoking large grains or high dust-to-gas ratios.

Spherical model bias: Spherical-grain models underestimate far-IR fluxes unless additional dust mass is assumed, biasing dust and massloss estimates of dust content.

Composition dependence: Continuum variations are driven by dust absorptivity and thus by grain composition. This is evident for graphite grains showing the strongest effects (see Fig 2).

Acknowledgements

This work was supported by Universidad Nacional Autónoma de México Postdoctoral Program (POSDOC). PJH and SJA acknowledge financial support from UNAM PAPIIT project IN109823. PJH, DG, OM and JM acknowledge support by grants PID2021-123370OB- 100 AEI/10.13039/501100011033/FEDER, PID2024-156713OB- I00/AEI/FEDER, and Severo Ochoa CEX2021-001131-S funded by MCIN/AEI/ 10.13039/501100011033. LS and PJH acknowledge fi- nancial support from UNAM PAPIIT project IN107625.

References

[1] Saito, M., Yang P., et al., 2021, Journal of the Atmospheric Sciences, 78, 2089

[2] Ferland, G. J., et al., 2017, RMxAA, 53, 385

[3] Hamann W. R., Grafener G., 2003, A&A, 410, 993